Spectral Phase-Encoded Time-Spreading (SPECTS) Optical Code-Division Multiple Access for Terabit Optical Access Networks

Vincent J. Hernandez, Yixue Du, Wei Cong, Ryan P. Scott, Kebin Li, Jonathan P. Heritage, *Fellow, IEEE*, Zhi Ding, *Fellow, IEEE*, Brian H. Kolner, *Senior Member, IEEE*, and S. J. Ben Yoo, *Senior Member, IEEE*

***Abstract*—This paper discusses design, simulation, and experimental investigations of optical-code-division multiple-access (O-CDMA) networking using a spectral phase-encoded time spreading (SPECTS) method. O-CDMA technologies can potentially provide flexible access of optical bandwidths in excess of 1 Tb/s without relying on wavelength- or time-division-multiplexing modules, provided that they overcome the interference caused by other users broadcasting over the same channel, called multiuser interference (MUI). This paper pursues theoretical and experimental methods to mitigate the MUI. Analysis shows that nonuniform phase coding can increase the orthogonality of the code set, thereby reducing the impact of the MUI. The experiment conducted in a SPECTS O-CDMA testbed incorporating a highly nonlinear thresholder demonstrated error-free operation for four users at 1.25-Gb/s/user and for two users at 10-Gb/s/user.**

***Index Terms*—Access networks, optical code-division multiple access (OCDMA), optical Internet, optical thresholding, phase modulation.**

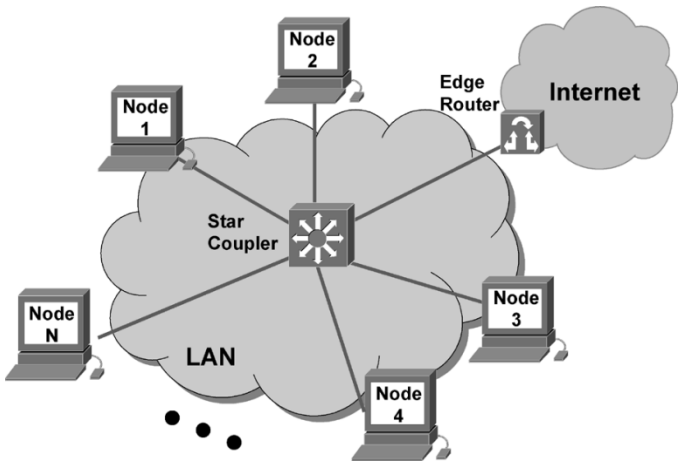

Fig. 1. Broadcast-and-select local area network using O-CDMA.

I. Introduction

DEMAND for high-capacity networking has promoted rapid deployment of both time-division multiplexing (TDM) and wavelength-division multiplexing (WDM) technologies in metro- and wide-area networks. While these require processing in the time and wavelength domains, optical-code-division multiple access (O-CDMA) is an alternate technology that allows multiple users to share bandwidth through encoded transmission. Each user is assigned a unique code that is part of an orthogonal (or quasi-orthogonal) set and thus users can transmit over the same bandwidth with minimal interference. When applied to current networks, O-CDMA has long been considered most advantageous in local area networks (LAN) that adopt a broadcast-and-select architecture owing to its simplicity and flexibility. Fig. 1 illustrates an example of such a network. Each end node encodes their signal and then broadcasts it to all others via a central star coupler. On the receiving end, each node receives the sum of the transmitted signals coming from all other nodes. To tune in to a particular broadcast, the receiver must know the code of the transmitter, and this is applied to the receiver's decoder. This allows the desired signal to become separable from all other broadcasts. To communicate outside of the LAN, nodes communicate to an edge router that converts O-CDMA signals to the protocol used in the outer network.

The actual implementation methods of O-CDMA vary [1], and most can be classified as using either direct sequence encoding or spectral encoding. Direct sequence encoding represents each bit as a spreading sequence of short pulses (sometimes referred to as "chips"), which may also be transmitted over different wavelengths [2]–[7]. Achieving sufficiently orthogonal code sets requires each bit to contain many time slots, and thus pulses need to be narrow enough to fit within the time slot. This becomes restrictive for higher data rates, since producing such narrow pulses becomes increasingly difficult. In contrast, spectral encoding is not constrained by TDM requirements, and thus more viable for high-speed networks. These schemes apply their codes through amplitude [8], [9] or phase modulation of a spectrum instead of in the time domain. One such spectral encoding scheme applies its code by phase modulating the spectrum of a femtosecond optical pulse. The phase encoding causes the femtosecond pulse to spread out in time and to appear as a noise-like burst, and thus this is called spectral phase-encoded time-spreading (SPECTS) O-CDMA. SPECTS O-CDMA systems have been previously reported [10], [11], but

Manuscript received January 27, 2004; revised July 9, 2004. This work was supported in part by DARPA and SPAWAR under agreement N66001-02-1-8937 and in part by the AFOSR through the University of California, Davis, Center for Digital Security.

V. J. Hernandez, Y. Du, K. Li, J. P. Heritage, Z. Ding, and S. J. B. Yoo are with the Department of Electrical and Computer Engineering, University of California, Davis, CA 95616 USA (e-mail: yoo@ece.ucdavis.edu).

W. Cong, R. P. Scott, and B. H. Kolner are with the Department of Applied Science, University of California, Davis, CA 95616 USA.

Digital Object Identifier 10.1109/JLT.2004.836752

few have taken advantage of its high data rate possibilities, generally operating under 1 Gb/s. One system that did operate at 10 Gb/s featured only one user [12], and thus failed to investigate interference effects that would come from multiple users in a broadcast-and-select network. This multiuser interference (MUI) greatly degrades the quality of the desired transmission and must be resolved to make SPECTS O-CDMA viable for realistic high-capacity network applications. In this paper we investigate methods to mitigate this MUI in a 10-Gb/s system. As a review, we first give an overview of the SPECTS O-CDMA operating principle (Section II), and then we propose a method called nonuniform coding to improve the contrast between MUI and a desired signal (Section III). Afterwards, we present a 10 Gb/s SPECTS O-CDMA testbed that uses a second encoder as an MUI source (Section IV). It utilizes a highly nonlinear thresholder to separate the desired signal from the MUI after decoding. Results are compared between two different coding schemes, Walsh codes and m-sequences. Section V concludes the paper.

II. SPECTS O-CDMA Operating Principle

SPECTS O-CDMA is based on the concept of pulse shaping, where the envelope of a pulse is manipulated by applying different phase shifts to different portions of the pulse's spectrum [13], [14]. Encoding occurs when the applied phase shifts cause a femtosecond pulse to appear as a noise-like burst, and decoding occurs by applying the inverse phase shift to the burst, thereby recovering the original pulse. The potential for O-CDMA results from having multiple encoders transmitting simultaneously, each assigned their own code that produces minimally interfering noise bursts. Then, in a network, many encoded pulses can coexist over the same channel and the total bursts appear as background noise to unauthorized receivers. Only receivers that contain the proper decoder can recover the original pulse, and its peak will rise above the noise floor of the other users. A thresholder ultimately allows this peak to be extracted.

Fig. 2 shows the setup of a pulse shaper, traditionally implemented with bulk optic components. When used as an encoder, the input is a femtosecond pulse $e_{\text{in}}(t)$, which contains a very wide spectrum due to its short width. To access the spectrum, denoted as $E_{\text{in}}(\omega)$, a diffraction grating is placed in its path, allowing the frequency components to disperse in space. The grating essentially performs a Fourier transform on the pulse, since one can now operate on the pulse in the spectral domain. A lens focuses the dispersed frequency components onto the phase shifter. The phase shifter contains an array of pixels, and each pixel applies a designated phase shift to the spectral components that pass through. Often, phase shifters are implemented with a spatial light phase modulator (SLPM), whose pixels consist of a liquid crystal. Applying an electrical voltage to the crystal causes a change in optical path length, resulting in a phase change. The phase function is denoted as $M(\omega)$, and contains the code. After phase modulation, the spectral components are recombined with another lens and grating to produce the new modified pulse, which can be defined as

$$e_{\text{out}}(t) = F^{-1}\left(M(\omega)E_{\text{in}}(\omega)\right)$$

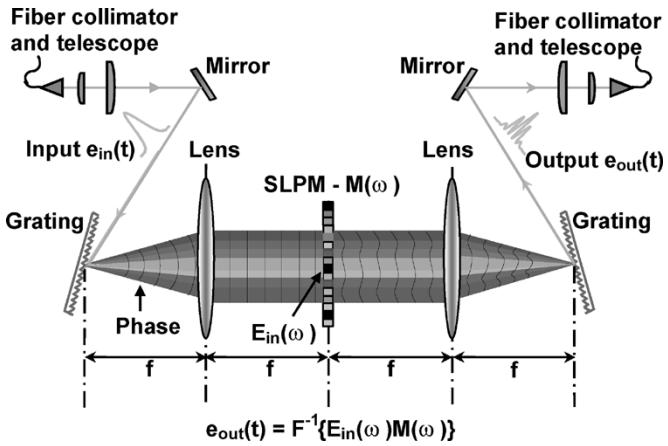

Fig. 2. Femtosecond pulse shaper used as an encoder or decoder for SPECTS O-CDMA. Phase encoding is performed using a spatial light phase modulator (SLPM).

where F^{-1} denotes the inverse Fourier transform. The end result $e_{\text{out}}(t)$ appears as a noise-like burst in the case of the encoder. The same setup may be used as a decoder, in which case $e_{\text{in}}(t)$ is the noise burst and $M^{-1}(\omega)$, the inverse phase code, is used by the SLPM. In this scenario, $e_{\text{out}}(t)$ reproduces the initial pulse into the encoder. If the phase coding in the encoder is not equal to $M^{-1}(\omega)$, the mismatched decoder will produce a distorted pulse. Through the use of orthogonal (pseudoorthogonal) codes, an ideal (nearly ideal) situation occurs where the distorted pulse appears as another noise burst that produces minimal (small) MUI. The next section further discusses coding and presents a new method for improving the effectiveness of the code.

III. Nonuniform Spectral Encoding for SPECTS O-CDMA

The original SPECTS O-CDMA analysis [15] assumed that optical pulses had flat spectral shapes (uniform spectral power density). In this case, encoding occurred by dividing the spectrum into equal portions of frequency, called chips, and applying a different phase shift to each portion. Since each chip contained an equal amount of energy, this led to near orthogonality between multiple access users and near perfect MUI suppression. To deal with a more realistic pulse spectrum, this section proposes a new coding scheme that adjusts the width of each frequency chip according to the actual nonflat spectral shape pulses in the O-CDMA system. Further, it demonstrates that this new coding method significantly improves the orthogonality in the optical phase coding and reduces the impairments due to the MUI, resulting in reduced bit-error rates (BERs) for a given number of simultaneous users or an increased number of users for a given BER.

A. Uniform Versus Nonuniform Phase Coding in SPECTS O-CDMA

We first approximate the ultrashort pulse by a Gaussian-shaped pulse whose time-domain electrical field is

$$E(t) = E_0 \exp\left[-\frac{1}{2}\left(\frac{t}{\tau}\right)^2\right]. \tag{1}$$

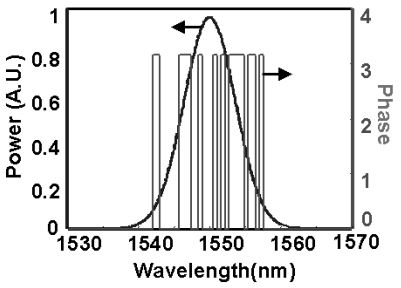

(a)

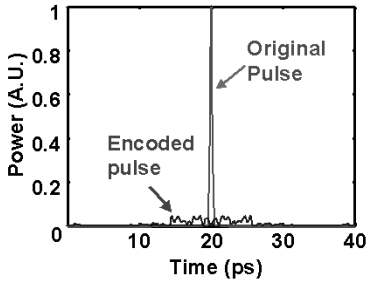

(b)

Fig. 3. (a) Phase encoding with the 31-chip m-sequence across the pulse spectrum. (b) The time domain optical pulse of the original and the encoded pulses.

Here E_0 is the normalized peak amplitude of the pulse, and the corresponding spectrum distribution is also Gaussian. The entire pulse spectrum is divided into various frequency chips, where the total number of chips is chosen to be the length of the selected phase code. As an example, a 31-chip m-sequence is used as the basic spreading code. Each user then employs a cyclically shifted version of such a binary code as its phase code, where "1" and "0" phase codes represent phase shifts of 0 and π, respectively. Fig. 3(a) illustrates the induced phase shift across the spectrum according to the m-sequence.

The amplitude of the electric field of the transmitted signal pulse can be written in its discrete Fourier series form as

$$E(n) = \sum_{k=-N}^{N} E_k \exp\left[-j\frac{2\pi n}{N}k\right]. \tag{2}$$

After encoding (applying encoding phase shift $\varphi^e(k) = 0, \pi$ to each chip), the encoded electric field becomes

$$E(n) = \sum_{k=-N}^{N} E_k \exp\left\{-j\left[\frac{2\pi n}{N}k + \varphi^e(k)\right]\right\}. \tag{3}$$

Fig. 3(b) illustrates that the encoded pulse is transformed into a time-spread pulse with lower peak power after the encoding compared to the original pulse, while maintaining the integrated optical pulse energy. The decoder is similar to the encoder but adds another phase shift ($\varphi^d(k) = 0, \pi$) to each frequency chip, yielding the decoded electric field

$$E(n) = \sum_{k=-N}^{N} E_k \exp\left\{-j\left[\frac{2\pi n}{N}k + \varphi^e(k) + \varphi^d(k)\right]\right\}. \tag{4}$$

By applying decoding phase shifts that are conjugate to the encoding phase shifts for all frequency chips, i.e., $\varphi^d(k) = -\varphi^e(k)$ for all k, one can reconstruct the original pulse of (2). If this is not the case, i.e., $\varphi^d(k) \neq -\varphi^e(k)$ for any k, then the correct decoding will not occur. Limiting the set of coding to within the nearly orthogonal codes, the incorrectly decoded output will continue to have low peak power and a wide time spread. Even though multiple users share the optical channel over a common fiber link, only the desired receiver can receive the correctly decoded signal while all other users will see incorrectly decoded signals that behave like noise.

The orthogonality of codes affects MUI in O-CDMA networks. Since signals sent out from different users share the same fiber link and will reach every user in the shared network, the signals will interfere with each other, often strongly enough to cause receiving errors. If we take into consideration the random polarization and phase delay of each fiber connection, the total electrical field of the MUI at the ith receiver can be expressed in its transverse-electric (TE) and transverse-magnetic (TM) components as

$$\begin{aligned} E_{k_\mathrm{P}} &= \sum_{\substack{m=1\\ m\neq i}}^{M} \sum_{k=-N}^{N} E_{k,m} \exp\left\{-j\left[\frac{2\pi n}{N}k + \varphi_m^e(k) + \varphi_i^d(k)\right]\right\} \\ &\quad \times \exp(j\phi_m)\cos(\theta_m) \\ E_{k_\perp} &= \sum_{\substack{m=1\\ m\neq i}}^{M} \sum_{k=-N}^{N} E_{k,m} \exp\left\{-j\left[\frac{2\pi n}{N}k + \varphi_m^e(k) + \varphi_i^d(k)\right]\right\} \\ &\quad \times \exp(j\phi_m)\sin(\theta_m) \end{aligned} \tag{5}$$

where M is the total number of cochannel users, ϕ_m is the random phase delay for each user, and θ_m indicates the polarization direction. For high-performance O-CDMA networks, the selected set of codes $\varphi^{e,d}$ must yield low MUI. As shown in [15], [16], with a flat spectrum for the signal ($E_{k,m}$ constant for all k), one can factor out $E_{k,m}$ from the double summation; therefore, by selecting an orthogonal code set of φ^e and φ^d, one can make the interference zero. In the practical case of nonuniform spectral shape pulses, $E_{k,m}$ is not constant and cannot be factored out of the double summation. Thus, the application of a similar encoding method will yield poor orthogonality, resulting in much more severe MUI effects. This proposed new encoding method will adjust frequency chip intervals so that the area (integrated power) of each chip under the spectral shape is approximately constant. Fig. 4(b) illustrates this in contrast to the uniform spectral case of Fig. 4(a).

B. Performance Comparison of Uniform Coding Versus Nonuniform Coding SPECTS O-CDMA

Simulations on the two coding methods adopted a Gaussian-shaped pulse with a full-width at half-maximum (FWHM) of approximately 500 fs. Cyclically shifted 31-chip m-sequences were employed for the phase codes and encoded pulses were detected using a nonlinear threshold detector (see Section IV-B). For uniform phase coding, each chip contains 75 GHz, covering 95% of the total spectral power. The remaining 5% of spectrum remains uncoded and is filtered out. The resulting BER simulations show that a system using this scheme can achieve

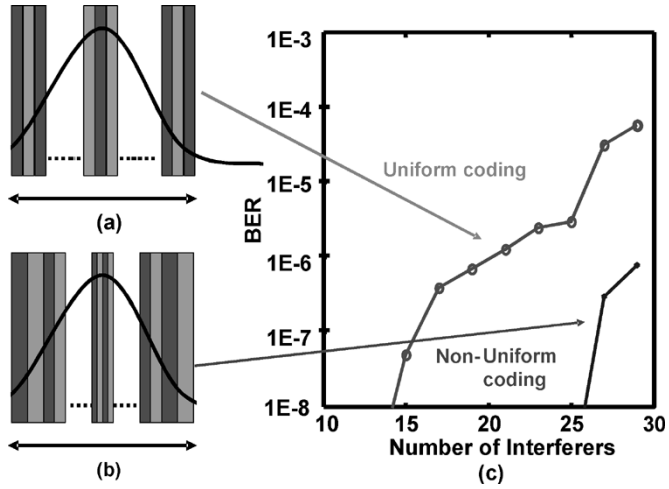

Fig. 4. Illustration of (a) a uniform coding scheme versus (b) a nonuniform coding scheme and (c) a comparison of their simulated BERs.

BER's of less than 1E-8 for 14 simultaneous users [Fig. 4(c)]. For ideal nonuniform coding, the width of each chip must be adjusted such that all chips contain the same power level, thus achieving complete spectral equalization. We consider a simpler case in which the total coded spectrum will have three different chip sizes. The central two-thirds of the encoded spectrum has 50-GHz chip widths, the surrounding one-sixth has 100-GHz chip widths, and the outer one-sixth has 150-GHz chip widths. The number of chips remains at 31 and only 95% of the total spectrum is encoded. Fig. 4(c) compares the BER for uniform and nonuniform coding schemes at 10-Gb/s data rates, and shows that the O-CDMA system can accommodate 25 simultaneous users in the nonuniform coding case as compared to only 14 for the uniform case at 1E-8 BER. In summary, this simulation study indicates that nonuniform phase coding provides a significant improvement by accommodating twice as many users in the O-CDMA network compared to the case of uniform phase coding for a given BER level of 1E-8.

IV. SPECTS O-CDMA Testbed

This section presents a 10-Gb/s SPECTS O-CDMA testbed that features MUI emanating from a second user. Although a slower system [17] (550 MHz) has demonstrated this MUI, it only encodes the interferer and does not feature a decoder. It assumes that the direct output of a mode-locked laser represents the properly decoded pulse of the desired signal. The testbed described here is the first one to our knowledge that operates at 10 Gb/s with both signal and interferer going through encoders and a decoder, and the first one to demonstrate a 10-Gb/s thresholder, which is key to suppressing the MUI. Section IV-A gives an overview of the testbed, and Section IV-B provides a description of this thresholder. Section IV-C. shows the combined results of the testbed and thresholder. Results using Walsh and m-sequence coding schemes, and the merits of each coding scheme, are compared in this section.

A. Testbed Overview

Fig. 5 shows the experimental setup for the SPECTS O-CDMA testbed, including three subsystems: the mode-locked laser, the encoders and decoders, and the thresholder discussed in the next section. The mode-locked fiber laser system (Pritel UOC-3 and Pritel FP-300) generates femtosecond pulses and is composed of an optical clock, an erbium-doped fiber amplifier (EDFA), and a pulse compressor. The optical clock produces pulses with a FWHM of 2.4 ps at a 10-GHz repetition rate. To reduce the temporal pulse width, the EDFA amplifies the pulse to produce significant soliton and nonlinear effects inside the pulse compressor, which contains proprietary specialty fiber, to generate 430-fs FWHM pulses. The mode-locked laser provides femtosecond pulses to four encoders by optically splitting them, where one encoder is designated as the desired signal source and the others are designated as the source of multiuser interference. Each encoder pulse stream is on-off keyed with a pseudorandom bit sequence (PRBS) using a single Mach–Zehnder $LiNbO_3$ modulator. To effectively emulate uncorrelated multiple PRBS sequences on each encoder, a set of a fixed time delay lines and a variable delay line applies bit shifts to each of the interferer paths. The encoder outputs are power balanced using variable attenuators before getting combined into a single dispersion compensated EDFA that leads to the decoder, and eventually the thresholder. The signal encoder and decoder have complementing phase codes, which will result in proper pulse decoding. The interferer encoders contain codes orthogonal to the decoder, and thus they will not produce correctly decoded pulses.

The encoders and decoder follow the operating principle in Section II, where the pulse shapers begin and end with fiber pigtailed collimators to transfer the pulses between the fiber and free space domain. The collimators produce a 1.6-mm-diameter beam that is expanded with a telescope to 12.8 mm. The increased beam diameter ensures sufficient spectral spreading when the beam is incident at $\sim$ 65° onto a 1100 lines/mm diffraction grating. The dispersed components diffract at $\sim$ 53° and a lens with focal length of 500 mm focuses the components toward an SLPM. The SLPM is a Cambridge Research CRI-128 that contains an array of 128 100 μm $\times$ 2 mm pixels, where each pixel can be electronically programmed to modulate up to 4π phase delay. The spectrum components are recombined using another lens and grating positioned symmetrically with the initial lens/grating pair.

Pulses produced by the system are shown in Figs. 6 and 7. The cross-correlation trace in Fig. 6(a) shows that the FWHM of the mode-locked laser pulses after compression is approximately 430 fs assuming a Gaussian pulse shape. Fig. 6(b) shows the spectral shape manifesting the effects of self-phase modulation produced by the pulse compressor. 90% of its bandwidth is within 10 nm (1.2 THz) of the central wavelength of 1550 nm (193 THz). When it passes through the encoder without applying a phase code, the SLPM within the encoder acts as an aperture that clips the spectrum at wavelengths less than 1545 nm and greater than 1565 nm. The passed spectrum also indicates that the loss through the SLPM is nonuniform; attenuations at the outer wavelengths are greater than at 1550 nm. Fig. 6(c) shows the temporal pulse output when a code is applied to the encoder. The figure contains two output traces, one is from applying a 31-chip length m-sequence phase code and the other is from using a 32-chip Walsh code. In both cases, every

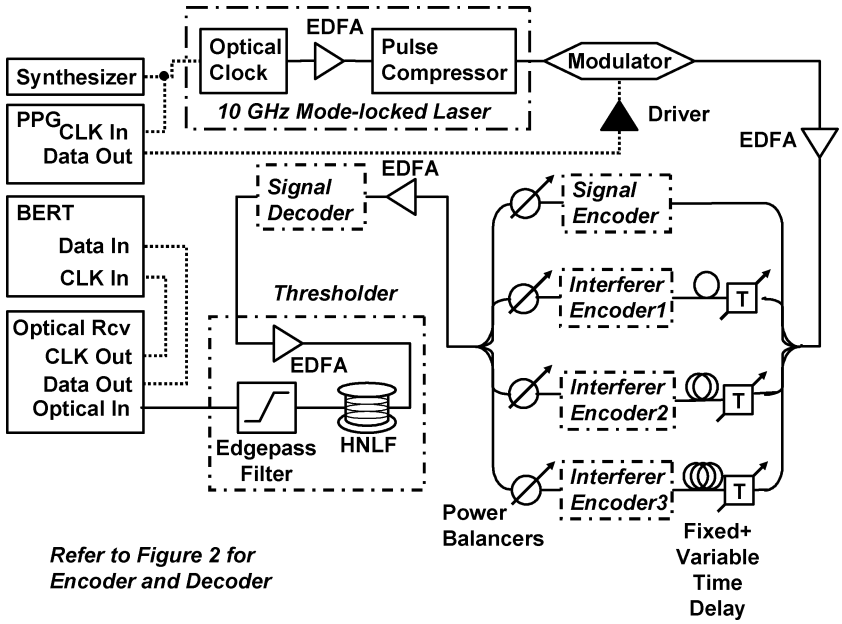

Fig. 5. Schematic of the SPECTS O-CDMA testbed with multiple interferers. Components include a pulse pattern generator (PPG), a bit-error rate tester (BERT), dispersion compensating fibers (DCF), EDFA, a thresholder module consisting of an EDFA, a highly nonlinear fiber (HNLF), and an edge- or long-pass filter. The mode-locked laser with a pulse compressor emits optical pulses that will split in four separate paths, each of which will be delayed and phase encoded to emulate a signal and three interferers with independent pseudorandom data bit sequences. The fixed time delay lines and the variable time delay lines achieve the data bit delays with fine adjustments.

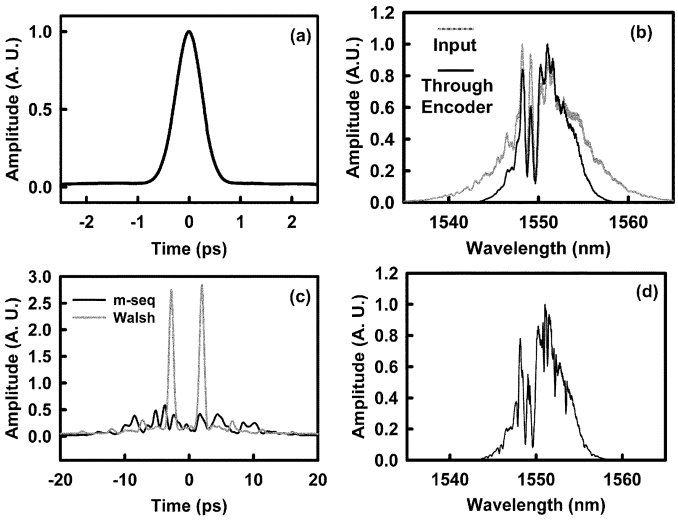

Fig. 6. Cross-correlation traces and spectra showing the optical pulse state at various points in the system: (a) output pulse of the mode-locked laser, (b) spectrum of mode locked laser pulse (gray) and spectrum of pulse through encoder with no phase code applied (black), (c) encoded pulse with a 31-chip m-sequence (black) and 32-chip Walsh code (gray), and (d) spectrum of encoded pulse.

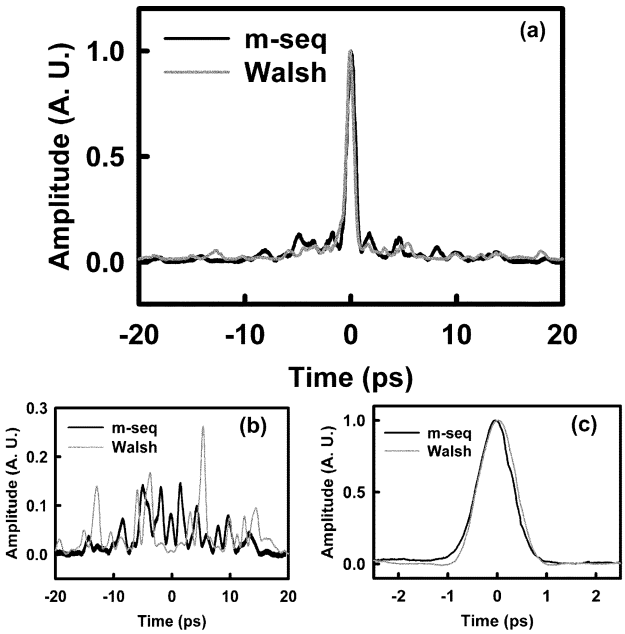

Fig. 7. Cross-correlation traces showing the decoded output of (a) both decoded signal and interferer, (b) interferers only, and (c) decoded signals only using m-sequences (black) and Walsh codes (gray).

four adjacent pixels of the SLPM represent one chip of the code. The transitions between 0 and π phase shifts manifests itself as gaps in the spectrum shown in Fig. 6(d). The coding has caused the pulse to produce a noise burst approximately 30 ps in width, or almost one hundred times longer than the original pulse. Due to the distribution of power in time, the encoded pulse has peak intensity 10 times lower than the original pulse. Fig. 7 shows the resulting optical output of encoded pulses passing through the decoder. The temporal trace in Fig. 7(a) shows the combined signal from the intended user and an interferer after passing through the decoder. Despite the interference, the trace shows a sharp spike at the center, indicating a strong contrast. The decoder reproduces the signal pulse while the interferer remains as a noise-like burst. Traces obtained for the m-sequence and Walsh codes appear very similar. Fig. 7(b) and (c) shows closer views of the decoded interferer and decoded signal separately by themselves for both m-sequence and Walsh coding schemes. When the correct phase code is applied, the recovered pulses have FWHM of 580 and 610 fs for m-sequences and Walsh

codes, respectively. The increases in the temporal pulse widths after the encoding and decoding are due to imperfect dispersion compensation in the system and pulse distortion caused by the spectral clipping of the SLPM.

B. 10-Gb/s Highly Nonlinear Thresholder

The ability to successfully discriminate between correctly and incorrectly decoded pulses remains one of the key challenges in femtosecond pulse O-CDMA. Even though an incorrectly decoded pulse broadens considerably compared to a correctly decoded pulse, typical optical receivers cannot differentiate them because of limited temporal responses. An incorrectly decoded pulse in the testbed above, although it spreads from 410 fs to 30 ps, is still well within the temporal response of a 10-Gb/s receiver with a 100-ps bit time. Therefore, both correctly and incorrectly decoded optical pulses will yield nearly indistinguishable output responses on the 10-Gb/s receiver. Even a 40-Gb/s receiver with temporal response at 25 ps will barely show any difference, mandating the need for nonlinear power thresholding rather than simple square-law integration in typical photoreceivers. Many thresholders have been implemented to reject incorrectly decoded pulses [18]–[20], but none has been used for multigigabit-rate applications. One of the simplest of these schemes utilizes nonlinearities in optical fibers [18], and we have modified this scheme to operate at 10 Gb/s with lower pulse energy levels by adding a highly nonlinear fiber (HNLF), as shown in Fig. 5. The thresholder in [20] used dispersion-shifted fiber (DSF) where the DSF's zero-dispersion wavelength is near the central wavelength of the pulse spectrum. Pulses that travel through the DSF generate additional frequency components through self-phase modulation, and a filter passes these additional components through to a receiver. An EDFA precedes the DSF in order to strongly drive the nonlinear optical effects. Thresholding occurs because only a correctly decoded pulse, with concentrated peak power, can induce the nonlinear effects that generate the shifted frequency components. The noise burst of an improperly decoded pulse will not have enough peak power to induce substantial self-phase modulation, even after the EDFA. Experiments using the DSF-based nonlinear thresholder [17], [21] operated with 480-fs pulses at a repetition rate of only 40 MHz, yielding peak powers of approximately 13 W for an average power of 250 μW. The O-CDMA testbed described in this paper requires even higher sensitivity (lower peak power detection), with a 10-GHz repetition rate, peak powers of 7.7 W, average powers of up to 31.6 mW, and 410-fs pulsewidths. The O-CDMA testbed incorporates a 500-m-long HNLF (Sumitomo Electric), achieving 1.7 times more sensitivity than in previous reports [17], [21]. Compared to the thresholder in [19], the HNLF thresholder requires higher power, but provides polarization independent detection.

Fig. 8 illustrates the operation of the highly nonlinear thresholder, using a HNLF with zero dispersion wavelength at 1543 nm, dispersion of 0.19 ps/nm/km at 1550 nm, dispersion slope of 0.026 ps/nm^2/km at 1550 nm, effective area of 10 μm^2, and nonlinear coefficient of 20 (W km)$^{-1}$. An encoded pulse spectrum is shown to have its peak power centered at 1553 nm, and the majority of its power lies between 1545 and 1560 nm. Spectrum components at wavelengths greater than 1560 nm are at least 15 dB lower than the components centered at 1553 nm. Power contained in wavelengths below 1545 nm comes from amplified spontaneous emission (ASE) from the EDFA, peaking at 1530 nm. When this pulse is properly decoded, self-phase modulation causes the power from the central peak to shift to higher and lower wavelengths, with significant power concentrated around 1545 and 1570 nm. A long-pass filter with a 1568-nm cutoff wavelength allows the longer wavelength components to pass through to the detector, and the total power for the correctly decoded pulse shows at least a 23-dB contrast ratio when compared to the incorrectly decoded pulse. This highly nonlinear thresholder is used to reject multi-user interference, as shown in the following subsection.

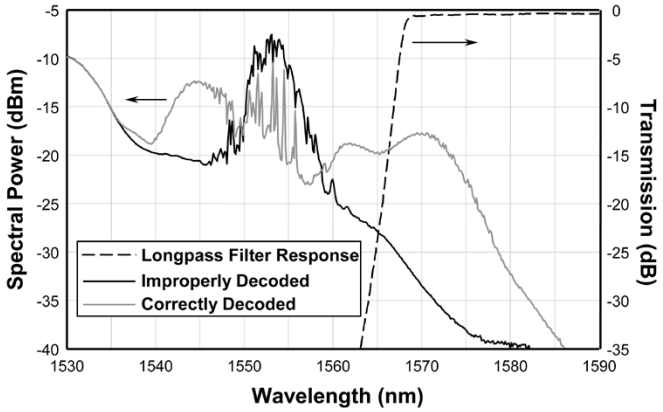

Fig. 8. Spectral results of the HNLF-based nonlinear thresholder showing the output for an incorrectly decoded pulse (black line), the output for a correctly decoded pulse (gray line), and the response of the long-pass filter (dashed line)

C. Multiuser Interference Results

This subsection discusses experimental results from the SPECTS O-CDMA system with interferers obtained for 10-Gb/s data rates with m-sequence codes and Walsh codes, and for 1.25-Gb/s data rates with Walsh codes.

Fig. 9 shows the BERs that result from the SPECTS O-CDMA system using m-sequences, showing curves and eyes for the following cases: (a) optical back-to-back, (b) single user, (c) asynchronous two-user, (d) and synchronous two-user. The BERs were measured using a $2^{31} - 1$ length PRBS, with the thresholder being included as part of the O-CDMA receiver. In other words, the horizontal axis on the BER plots indicates the total average optical power received in front of the O-CDMA receiver which includes the EDFA, the HNLF, the long-pass filter, and the photoreceiver. With the exception of (d), all cases achieve error-free performance (BER $< 10^{-12}$). The optical back-to-back is defined as the case where no encoder or decoder is present in the system. In the single user case, pulses pass through the signal encoder and these are properly decoded before going through the thresholder. There is a 4-dB penalty at BER $= 10^{-9}$ when compared to the back-to-back case. This results from the residual pulse widening caused by dispersion and spectral clipping in the pulse shapers. This increase results in a lower peak power, and this means that less spectral components are generated in the HNLF to pass

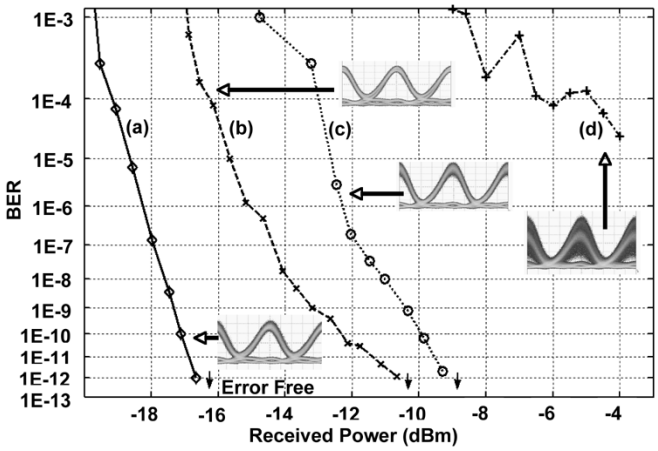

Fig. 9. BER measurement using the nonlinear thresholder with inset eye diagrams using 31-chip m-sequences. (a) Back-to-back. (b) No interferer. (c) With an asynchronous interferer. (d) With a synchronous interferer.

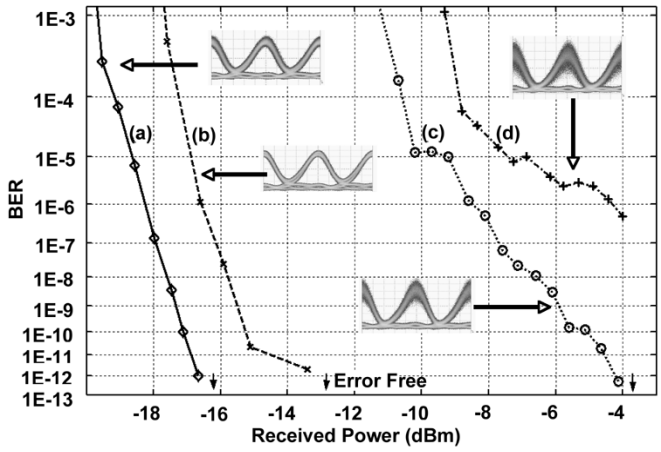

Fig. 10. BER measurement using the nonlinear thresholder with inset eye diagrams using 32-chip Walsh codes. (a) Back-to-back. (b) No interferer. (c) With an asynchronous interferer. (d) With a synchronous interferer.

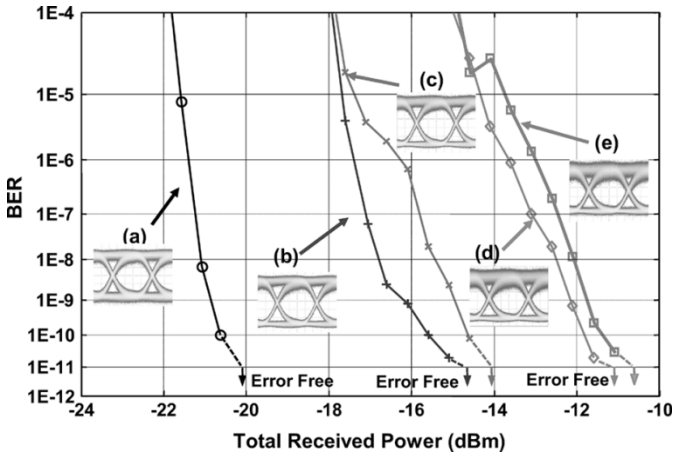

Fig. 11. BER measurement using the nonlinear thresholder with inset eye diagrams using 64-chip Walsh codes and 1.25-Gb/s data rate. (a) Back-to-back. (b) No interferer. (c) With a synchronous interferer.

into the receiver. Attempts were made to measure BER's in the case when the encoded pulse is improperly decoded, but due to the proper operation of the thresholder, the BER values stayed close to 0.5 with the available power. The effectiveness of the thresholding is further illustrated in the asynchronous two-user case. Here, both signal encoder and interference encoder send their pulses to the decoder, but their pulses are misaligned by 23 ps. This case can achieve error free operation, showing that the thresholder is correctly rejecting the pulses from the interferer. The 3-dB penalty compared to the single user case results only because the EDFA preceding the decoder must share its gain between two encoders. This case is representative of a network where two users transmit over the fiber asynchronously, such that the pulses from the interferer do not align with the pulses of the desired signal. Of course, in an asynchronous scheme, it is still possible for pulses from separate users to randomly align, and this scenario is also equivalent to a synchronous scheme. Both of these situations are considered in the synchronous two-user case. In this configuration, the pulse position of the interferer has zero delay with respect to the desired signal's pulse. When aligned in this way, optical coherent interference impacts performance as well as MUI, since both the desired signal and MUI are generated using the same mode-locked laser source. Hence, this case achieved BER $> 10^{-5}$. In a practical network, each user is expected to use its own laser, and a significant improvement is expected from lowered coherent crosstalk.

Fig. 10 shows equivalent BER curves using Walsh codes. There is a 2-dB penalty at BER $= 10^{-9}$ between the back-to-back case and the single user case. When adding the asynchronous interferer (misaligned by 18 ps), a 9.5-dB penalty occurs. This penalty is greater than when using m-sequence coding, and this is probably caused by residual energy from the decoded interferer. This energy varies depending on the code, and in this case it causes interference that is small enough to allow an error-free BER. For the synchronous case, BER $< 10^{-6}$ can be achieved, an order of magnitude better than the m-sequences. This improvement results from the amount of interference energy coincident with the desired signal. From Fig. 7(b), the Walsh code clearly yields lower optical intensity for the interferers at the center of the optical pulse (0 ps) compared to the m-sequence code, and thus allows for lower BER. Again coherence effects still restrict us from reaching error-free performance.

Using a lower bit rate and a longer code mitigates the coherence between the interferer and signal. Fig. 11 illustrates BER curves using a 1.25-Gb/s data rate and 64-chip Walsh codes measured for (a) back-to-back, (b) no interferer, (c) one synchronous interferer, (d) two synchronous interferers, and (e) three synchronous interferers. In all cases, the O-CDMA system achieves error-free (BER $< 10^{-12}$) performance. The downward arrows in Fig. 11 indicate the corresponding power levels where the BER measurements yielded no errors after receiving more than 3×10^{12} bits. In the experiment, the pulse pattern generator modulates the 10-GHz pulse train of the mode-locked laser with 1.25-Gb/s data, so that every eight optical pulses represent one data bit. The receiver, with a 933-MHz low-pass RF filter, recovers the 1.25-Gb/s data. Since the number of interferers range from 0 to 3, the gain of the EDFA inside the thresholder is adjusted such that the desired

signal always has a constant average power of 14 dBm going into the HNLF. Thus, the total average output power of the EDFA is 17, 18.8, and 20 dBm when respectively adding one, two, and three interferers. Compared to the single user case with no interferer, the BER measurements correspondingly show system power penalties of 0.8, 3.9, and 4.1 dB at BER $= 10^{-9}$. Of these penalty levels, 3, 4.8, and 6 dB can be attributed to the gain sharing of the EDFA between the encoder and decoder. The remaining -2.2, -0.9, and -1.9 dB are possibly due to adaptation of the EDFA gain level in the thresholder module coupled with the nonlinear response of the HNLF detection scheme. Improved BER performance and reduced MUI effects in the 1.25-Gb/s O-CDMA system compared to the 10-Gb/s system are likely to be due to the reduced coherent noise effects in the lower bit rate system. The coherent noise effects are expected to be significantly lower if each enconder is equipped with its own synchronized mode-locked laser source. The system overall is equivalent to a synchronous Gigabit Ethernet system operating over O-CDMA.

The difference in energy distribution of the improperly decoded pulse produced by the codes determines the codes' advantage in synchronous versus asynchronous O-CDMA schemes. The code used in Fig. 7(b) is atypical, but Walsh codes typically concentrate their energies into a few prominent peaks, with most having appearance more similar to Fig. 6(c). This is very disadvantageous in an asynchronous scheme, since it is possible for the desired signal to coincide with one of the peaks, resulting in dramatic multi-user interference. In contrast, the energy distribution caused by m-sequences is generally evenly distributed across the time spread. The multi-user interference is much less pronounced than a Walsh code pulse, and thus m-sequences are the preferred code to use in an asynchronous scheme. In a synchronous scheme, Walsh codes have the advantage since the produced peaks of an encoded pulse are always time shifted with respect to the decoded pulse. Since all energy is contained within these peaks, no MUI is coincident with the desired signal. Note that in Fig. 7(c), some residual power can still be seen in the Walsh codes, especially at the center. Some of this results from the aperture effects caused by the SLPM and loss of orthogonality due to uniform coding. Use of the nonuniform codes of Section III would improve the response.

The experiments so far included uniform coding, and nonuniform coding experiments are currently in progress utilizing variable width SLPMs. Simulation results in Fig. 4 indicate that the acceptable number of interferers increases from 14 to 25 at BER $= 10^{-8}$ when uniform coding was changed to nonuniform coding. The new experimental setup also includes phase modulators in the multiple user paths in order to break the coherence coming from using a single mode-locked laser source.

V. Conclusion

This paper presented a SPECTS O-CDMA testbed that contains MUI. The 1.25-Gb/s O-CDMA system successfully overcame the MUI effects and achieved error-free operation with low system penalty levels up to three synchronous interferers. The 10-Gb/s O-CDMA system achieved error-free operation up to one asynchronous intereferer but it showed error floors for a synchronous intereferer. Coherent interference appeared to affect synchronous operation, but improvements can be gained through proper selections of the O-CDMA code. Walsh codes demonstrated superior performance than m-sequences in the synchronous case, and the codes achieved synchronous error-free operation at 1.25 Gb/s. Even further improvement is expected with nonuniform coding, and analysis shows that the number of users in the O-CDMA system will nearly double when the applied code is tailored to the spectral shape of the pulse.

Acknowledgment

The authors wish to thank Sumitomo Electric for use of the highly nonlinear fiber and Pritel, Inc. for a loan of a high-power dispersion-compensated EDFA.

References

[1] N. Karafolas, "Optical fiber code division multiple access networks: a review," *Opt. Fiber Technol.*, vol. 2, pp. 149–168, 1996.

[2] P. R. Prucnal, M. A. Santoro, and T. R. Fan, "Spread spectrum fiber-optic local area network using optical processing," *J. Lightwave Technol.*, vol. 4, pp. 547–554, May 1986.

[3] M. E. Marhic, "Coherent optical CDMA networks," *J. Lightwave Technol.*, vol. 11, pp. 854–863, May 1993.

[4] R. M. H. Yim, L. R. Chen, and J. Bajcsy, "Design and performance of 2-D codes for wavelength-time optical CDMA," *IEEE Photon. Technol. Lett.*, vol. 14, pp. 714–716, May 2002.

[5] A. J. Mendez, R. M. Gagliardi, V. J. Hernandez, C. V. Bennett, and W. J. Lennon, "Design and performance analysis of wavelength time (W/T) matrix codes for optical CDMA," *J. Lightwave Technol.*, vol. 21, pp. 2524–2533, Nov. 2003.

[6] L. Tancevski and I. Andonovic, "Wavelength hopping/time spreading code division multiple access systems," *Electron. Lett.*, vol. 30, pp. 1388–1390, Aug. 1994.

[7] G.-C. Yang and W. C. Kwong, "A new class of carrier-hopping codes for code-division multiple-access optical and wireless systems," *IEEE Commun. Lett.*, vol. 8, pp. 51–53, Jan. 2004.

[8] M. Kavehrad and D. Zaccarin, "Optical code-division-multiplixed systems based on spectral encoding of noncoherent sources," *J. Lightwave Technol.*, vol. 13, pp. 534–545, Mar. 1995.

[9] Z. Wei, H. M. H. Shalaby, and H. Ghafouri-Shiraz, "Modified quadratic congruence codes for fiber Bragg-grating-based spectral-amplitude-coding optical CDMA systems," *J. Lightwave Technol.*, vol. 19, pp. 1274–1281, Sept. 2001.

[10] A. M. Weiner, J. P. Heritage, and J. A. Salehi, "Encoding and decoding of femtosecond pulses," *Opt. Lett.*, vol. 13, pp. 300–302, Apr. 1988.

[11] H. P. Sardesai, C.-C. Chang, and A. M. Weiner, "A femtosecond code-division multiple-access communication system test bed," *J. Lightwave Technol.*, vol. 16, pp. 1953–1964, Nov. 1998.

[12] H. Tsuda, H. Takenouchi, T. Ishii, K. Okamoto, T. Goh, K. Sato, A. Hirano, T. Kurokawa, and C. Amano, "Spectral encoding and decoding of 10 Gbit/s femtosecond pulses using high resolution arrayed-waveguide grating," *Electron. Lett.*, vol. 35, pp. 1186–1188, July 1999.

[13] J. P. Heritage, A. M. Weiner, and R. N. Thurston, "Picosecond pulse shaping by spectral phase and amplitude manipulation," *Opt. Lett.*, vol. 10, pp. 609–611, Dec. 1985.

[14] A. M. Weiner, "Femtosecond pulse shaping using spatial light modulators," *Rev. Sci. Instrum.*, vol. 71, pp. 1929–1960, May 2002.

[15] J. A. Salehi, A. M. Weiner, and J. P. Heritage, "Coherent ultrashort light pulse code-division multiple access communication systems," *J. Lightwave Technol.*, vol. 8, pp. 478–491, Mar. 1990.

[16] D. J. Hahela and J. A. Salehi, "Limits to the encoding and bounds on the performance of coherent ultra short light pulse code-division multiple access sytems," *IEEE Trans. Commun.*, vol. 40, pp. 325–336, 1992.

[17] S. Shen, A. M. Weiner, G. D. Sucha, and M. L. Stock, "Bit error rate performance of ultrashort-pulse optical CDMA detection under multi-access interference," *Electron. Lett.*, vol. 36, pp. 1795–1797, Oct. 2000.

[18] Z. Zheng, S. Shen, H. Sardesai, C.-C. Chang, J. H. Marsh, M. M. Karkhanehchi, and A. M. Weiner, "Ultrafast two-photon absorption optical thresholding of spectrally coded pulses," *Opt. Commun.*, vol. 167, pp. 225–233, Aug. 1999.
[19] Z. Zheng, A. M. Weiner, K. R. Parameswaran, M. H. Chou, and M. M. Fejer, "Low-power spectral phase correlator using periodically poled $LiNbO_3$ waveguides," *IEEE Photon. Technol. Lett.*, vol. 13, pp. 376–378, Apr. 2001.
[20] H. P. Sardesai and A. M. Weiner, "Nonlinear fiber-optic receiver for ultrashort pulse code division multiple access communications," *Electron. Lett.*, vol. 33, pp. 610–611, Mar. 1997.
[21] S. Shen and A. M. Weiner, "Suppression of WDM interference for error-free detection of ultrashort-pulse CDMA signals in spectrally overlaid hybrid WDM-CDMA operation," *IEEE Photon. Technol. Lett.*, vol. 13, pp. 82–84, Jan. 2001.

Vincent J. Hernandez was born in San Francisco, CA, in 1976. He received the B.S. and M.S. degrees in electrical engineering from the University of California, Davis, in 1999 and 2004, respectively. He is currently working toward the Ph.D. degree in optical communications at the same university, conducting part of his research in conjunction with Lawrence Livermore National Laboratory.

His current interest lies in developing optical code-division multiple-access technology.

Yixue Du received the M.S. degree in physics from Oklahoma State University, Stillwater, in 1998. She is currently working toward the Ph.D. degree in electrical engineering at the University of California, Davis.

Her research includes device simulation and testing in optical code-division multiple-access networks.

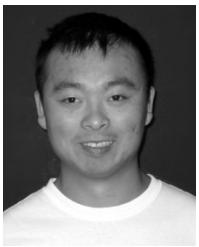

Wei Cong received the B.S. degree in physics from Jilin University, China, in 1999, and the M.S. degree in applied science from the University of California, Davis (UC Davis), in 2002. He is currently working toward the Ph.D. degree in applied science at UC Davis.

He is currently a Graduate Student Researcher in the Laser Electro-Optic Research Group (LEORG) at UC Davis. His research work includes optical communication and ultrafast pulse shaping.

Ryan P. Scott received the B.S. degree in laser electrooptics technology from the Oregon Institute of Technology, Klamath Falls, in 1991 and the M.S. degree in electrical engineering from the University of California, Los Angeles (UCLA), in 1995. He is currently working toward the Ph.D. degree in electrical engineering from UCLA while working in the Laser Electro-Optic Research Group (LEORG) at UC Davis. His current research interests include temporal imaging, precise measurement of laser amplitude and phase noise, and the development of optical code-division multiple-access technology.

Kebin Li, photograph and biography not available at the time of publication.

Jonathan P. Heritage (S'74–M'75–SM'89–F'90), photograph and biography not available at the time of publication.

Zhi Ding (S'88–M'90–SM'95–F'04), photograph and biography not available at the time of publication.

Brian H. Kolner (SM'03) received the B.S. degree in electrical engineering from the University of Wisconsin, Madison, in 1979 and the M.S. and Ph.D. degrees in electrical engineering from Stanford University, Stanford, CA, in 1981 and 1985, respectively.

He was a Member of the Technical Staff at Hewlett-Packard Laboratories, Palo Alto, CA, from 1985 to 1991, and in 1991, he joined the Electrical Engineering Department at the University of California, Los Angeles (UCLA), and became Vice Chairman for Undergraduate Affairs in 1993. At UCLA, he taught courses in microwave measurements, Fourier optics, and quantum mechanics and conducted research on space–time duality and temporal imaging. In 1996, he moved to the University of California, Davis, where he holds joint appointments in the Departments of Applied Science and Electrical and Computer Engineering. His current research interests are in temporal imaging, laser phase and amplitude noise, and terahertz spectroscopy.

Dr. Kolner was awarded a David and Lucile Packard Foundation Fellowship in 1991, and in 1996 and 2003, he served as Guest Editor for the IEEE JOURNAL OF SPECIAL TOPICS IN QUANTUM ELECTRONICS.

S. J. Ben Yoo (S'82–M'84–SM'97) received the B.S. degree in electrical engineering with distinction, the M.S. degree in electrical engineering, and the Ph.D. degree in electrical engineering with a minor degree in physics from Stanford University, Stanford, CA, in 1984, 1986, and 1991, respectively. His Ph.D. dissertation was on linear and nonlinear optical spectroscopy of quantum-well intersubband transitions.

Prior to joining Bellcore in 1991, he conducted research on nonlinear optical processes in quantum wells, a four-wave-mixing study of relaxation mechanisms in dye molecules, and ultrafast diffusion-driven photodetectors. During this period, he also conducted research on lifetime measurements of intersubband transitions and on nonlinear optical storage mechanisms at Bell Laboratories and IBM Research Laboratories, respectively. He was then a Senior Scientist at Bellcore, leading technical efforts in optical networking research and systems integration. His research activities at Bellcore included optical-label switching for the next-generation Internet, power transients in reconfigurable optical networks, wavelength interchanging cross connects, wavelength converters, vertical-cavity lasers, and high-speed modulators. He also participated in the advanced technology demonstration network/multiwavelength optical networking (ATD/MONET) systems integration, the OC-192 synchronous optical network (SONET) ring studies, and a number of standardization activities. He joined the University of California, Davis, as Associate Professor of Electrical and Computer Engineering in March 1999. He is currently the Branch Director of the Center for Information Technology Research in the Interest of Society (CITRIS). His current research involves advanced switching techniques and optical communications systems for the Next Generation Internet. In particular, he is conducting research on architectures, systems integration, and network experiments of all-optical label switching routers.

Prof. Yoo is a Senior Member of IEEE Lasers & Electro-Optics Society (LEOS) and a Member of the Optical Society of America (OSA) and Tau Beta Pi. He received the Bellcore CEO Award in 1998 and DARPA Award for Sustained Excellence in 1997 for his work at Bellcore.